Tracer Diffusion at the Glass Transition

Dietmar Ehlich and Hans Sillescu*

Institut für Physikalische Chemie der Universität Mainz, Jakob-Welder-Weg 15, D-6500 Mainz, West-Germany. *Received April 7, 1989; Revised Manuscript Received August 21, 1989*

ABSTRACT: Diffusion coefficients D of photoreactive dye molecules having different sizes and flexibilities were measured in the glass formers polystyrene (PS), poly(ethylstyrene) (PES), poly(methyl methacrylate) (PMMA), poly(ethyl methacrylate) (PEMA), polycarbonate (PC), and tri-α-naphthylbenzene (TNB). The D values were determined by forced Rayleigh scattering from the diffusive decay of holographic gratings in a range $\sim 10^{-17}$–10^{-7} cm^2 s^{-1}. At temperatures above the glass transition T_g, the D values could be fitted to the WLF equation of the matrix after introducing a coupling that depends upon tracer solute and matrix properties. At T_g, the D values of the same solute molecule in different glasses vary from 6.3×10^{-12} cm^2 s^{-1} in PC to 7.9×10^{-16} cm^2 s^{-1} in TNB. Above and below T_g, the temperature dependence of D is between that of the α- and the β-processes of mechanical relaxation. Physical aging of D was observed below T_g and could be quantitatively related with volume retardation.

I. Introduction

Diffusion in polymers was for a long time synonymous with the transport of small molecules investigated mostly by permeation or sorption techniques.[1,2] The measured diffusion coefficients D are typically in a range of 10^{-5}–10^{-10} cm^2 s^{-1} and have an Arrhenius-type temperature dependence with apparent activation energies E_A of about 5–20 kJ mol^{-1} where only for the slowest diffusants an increase of E_A is observed above the glass transition temperature T_g.[2] Clearly, this rapid transport is almost completely decoupled from the α-process causing the glass transition. However, one should expect that the coupling will increase with the size of the diffusant, which finally becomes a probe for monitoring the glass process. Some examples based on sorption experiments in polystyrene can be found in refs 3–6. However, these measurements were performed at temperatures well above T_g where the D values are in range above 10^{-10} cm^2 s^{-1}. The advent of holographic grating (forced Rayleigh scattering) techniques has made it possible to measure slow translational diffusion of photochromic dye molecules at the glass transition. Our first results[8,9] have yielded $D(T_g)$ values down to about 10^{-14} cm^2 s^{-1}. In further experiments by Wang and Zhang[10-12] effects of plasticization and physical aging were also studied by dye diffusion via the holographic grating technique. The results provide valuable information on the dynamics of polymer glasses above and below T_g.

One can easily show that even the small D value of 10^{-14} cm^2 s^{-1} amounts to sizable decoupling of probe diffusion from matrix molecular motion at T_g. Let us try to obtain a rough estimate of the self-diffusion coefficient D of a supercooled organic liquid at T_g, e.g., *o*-terphenyl, which is of similar size as our dye molecules. If the Stokes–Einstein relation $D_s = k_B T/6\pi\eta r$ is assumed to be valid at T_g (r being some "effective" molecular radius) one obtains $D_s(T_g)$ from the temperature dependence of the shear viscosity η. Traditionally, $\eta(T_g)$ is ascribed a value of $\sim 10^{12}$ Pa s,[13,14] which yields $D_s(T_g) \sim 10^{-20}$ cm^2 s^{-1} since $D_s(T) \sim 10^{-5}$ cm^2 s^{-1} at a temperature T where $\eta(T) \sim 10^{-3}$ Pa s. This is 5–6 decades below the value quoted above for dye diffusion in polymers at T_g. The important question whether the Stokes–Einstein equation is applicable at T_g will be discussed further below (see Figure 8).

The theory of diffusion in concentrated polymer solutions and polymer–plasticizer systems has been formulated in the framework of the free volume concept by Fujita[15] and elaborated further in a series of papers by Vrentas et al.[16-19] In the limit of low solute concentrations and in the vicinity of T_g their result can be written in the form of the Williams–Landel–Ferry (WLF) equation[13] for the solute diffusion coefficient relative to its value at T_g

$$-\log a_T = \log [D(T)/D(T_g)] = \frac{C'_{1g}(T - T_g)}{C'_{2g} + T - T_g} \quad (1)$$

where C'_{1g} and C'_{2g} are related to the corresponding WLF parameters of the matrix via the coupling parameters ξ and λ:

$$C'_{1g} = \xi C_{1g} \quad (2)$$

$$C'_{2g} = C_{2g} \quad \text{for} \quad T \geq T_g \quad (3a)$$

$$C'_{2g} = C_{2g}/\lambda \quad \text{for} \quad T < T_g \quad (3b)$$

ξ is interpreted as the ratio of the critical molecular volume v_s^* of the solute jumping unit over the critical molecular volume v^* of the (polymer) matrix jumping unit, $\xi = v_s^*/v^*$. An alternative interpretation of ξ will be given below in section III.4. The parameter $\lambda < 1$ describes the change in the free volume expansion coefficient attributed to the onset of the glass transition. The WLF equation is closely related to the Vogel–Fulcher–Tammann (VFT) equation.[13]

$$D(T) = D'_0 \exp\left(-\frac{B'_0}{T - T_\infty}\right) \quad (4)$$

$$B'_0 = \xi B_0 = \xi C_{1g} C_{2g} \ln 10 \quad (5)$$

$$T_\infty = T_g - C_{2g} \quad (6)$$

$$D'_0 = \delta D_0 \quad (7)$$

The third coupling parameter δ may be important in relating the D values of the probe molecules with a hypothetical diffusion coefficient of the matrix monomer

$$D_{\text{matrix}} = k_B T/\zeta_0 \quad (8)$$

where ζ_0 is the monomer friction coefficient, which can

0024-9297/90/2223-1600$02.50/0 © 1990 American Chemical Society

Table I
Characterization of Matrices Used for Tracer Diffusion Experiments

sample	P_n	$10^4\alpha_l/K^{-1}$	$10^4\alpha_g/K^{-1}$	$10^4(\alpha_f/B)/K^{-1}$	f_g/B	T_g/K
polystyrene (PS)	2600	5.6	1.9	5.6	0.032	373
oligostyrene (PS-20)	20	5.6	1.9	5.6	0.032	339
PS/TCP[a]	2600	5.0	1.8	4.9	0.028	342
poly(ethylstyrene) (PES)	580	5.3	3.0	4.7	0.032	355
poly(methyl methacrylate) (PMMA)	2600	5.7	2.5	6.3	0.033	394
poly(ethyl methacrylate) (PEMA)	990	5.7	2.9	3.1	0.028	342
poly(bisphenol A carbonate) (PC)	140[b]	5.7	2.9	4.8	0.027	423
tri-α-naphthylbenzene (TNB)	1	5.2	1.6	1.1	0.015	345

[a] PS with 10 wt % tricresyl phosphate. [b] P_w.

be obtained in glassy polymers from dynamic mechanical experiments (cf. Chapter 12B of ref 13). It should be noted that the Vogel temperature $T_\infty = T_g - C_{2g}$ is assumed to be the same for all probe molecules and the matrix. A basic assumption of the free volume theory is that the temperature dependence in eqs 1 and 4 originates from the increased thermal expansion found in glasses above T_g, which is attributed to the expansion of "free volume".[13] Thus, the "fractional free volume" $f = v_f/v_m$ defined as the ratio of the average free volume v_f over some molecular volume v_m is assumed to vary with temperature as

$$f = f_g + \alpha_f(T - T_g) \tag{9}$$

α_f being the difference of expansion coefficients above and below T_g and f_g the fractional free volume at T_g. Comparison with eqs 4–6 yields

$$C_{1g} = \alpha_f B_0/(f_g \ln 10); \qquad C_{2g} = f_g/\alpha_f \tag{10}$$

It should be noted that a size parameter

$$B = \alpha_f B_0 \tag{11}$$

of order one is usually introduced in the free volume theory,[13] which relates the geometrical molecular volume to the critical volume of the jumping unit discussed above.

The ad hoc assumption of eq 9 was modified in later developments of the free volume theory by Cohen and Grest.[20] However, further assumptions had to be introduced for describing the increased mobility in "liquid-like clusters" on increasing the temperatures. Adam and Gibbs[21] starting from a rather different conception arrive at an equation where the diffusion coefficient is given by

$$D = C \exp\left(-\frac{A}{TS_c(T)}\right) \tag{12}$$

C and A are constants and $S_c(T)$ is a configurational entropy that is related with the difference of heat capacity above and below T_g. In a temperature range up to about 50 K above T_g, eqs 1 and 12 yield almost the same temperature dependence. Recently, Bässler and Richert have discussed the validity of a "T^2-law"

$$D = D_\infty \exp(-T_0^2/T^2) \tag{13}$$

in a certain temperature range above T_g.[22–24] On the basis of particular assumptions for transport between states randomly distributed in space having a Gaussian energy distribution,[24] they arrive at a picture where, in effect, each molecule jumps over barriers corresponding to a Gaussian distribution of activation energies. This is closely related with the log-Gauss distribution of correlation times introduced by Wagner[25] in 1913, which was also discussed in terms of Gaussian environmental fluctuations[26] and a Gaussian distribution of activation energies.[27] Thus, the T^2-law is obtained from eq 5 of ref 27 in the limit of low temperatures or a large width of the energy distribution that was, however, not considered by these authors. Since the picture of diffusional transport by hopping over static barriers should be most appropriate for probe diffusion with variable coupling to the glass process, we shall compare our results with the predictions of eq 13, cf. Figure 4. At temperatures below T_g the dynamics is complicated through effects of *physical aging*.[28] For example, on rapid cooling of a sample to some temperature below T_g (typically 10–20 K) its volume $V(t)$ contracts during a long period of time resulting in a limiting value $V(\infty)$. From free volume theory, one should expect that $V(t)$ is related to the fractional free volume defined above by

$$V(t) = V(\infty) + V_f(t) - V_f(\infty)$$
$$\approx V(\infty)[1 + f(t) - f(\infty)] \tag{14}$$

where it is assumed that physical aging only affects the free volume $V_f(t)$ whereas the "occupied volume" $V(\infty) - V_f(\infty)$ remains constant. The assumption $f = V_f/V(\infty)$ differs only by a few percent from the definition $f = V_f/V$ given above. Since the probe diffusion coefficient D is related with the fractional free volume f through eqs 4–6 and 9–10, volume contraction should result in a corresponding slow down of diffusion. The relation between $D(t)$ and $V(t)$ can be derived from eq 4 by assuming that the limiting value $D(\infty)$, obtained after very long annealing at the aging temperature $T < T_g$, corresponds to the WLF parameters $C'_{1g} = \xi C_{1g}$ and $C'_{2g} = C_{2g}$ determined at temperatures above T_g. Thus, we have to assume $\lambda = 1$ in eq 3b since the state at $t \to \infty$ has the thermal volume expansion coefficient determined at $T > T_g$. The diffusion coefficient $D(t)$ is time dependent only through $C_{1g}(t)$ which is related to $f(t)$ by eqs 9–11. Thus, we obtain

$$\ln [D(t)/D(\infty)] = \xi B[1/f(\infty) - 1/f(t)] \tag{15}$$

$f(\infty)/B$ is a matrix property obtained from eqs 9 and 10 and dynamic mechanical experiments at $T > T_g$ (see Table I) whereas $D(\infty) = D(\mathrm{WLF})$ can be determined from diffusion measurements above T_g by extrapolation through eq 4. Thus, $f(t)/B$ can be determined from eq 15 by measuring $D(t)$, which allows for calculating $V(t)$ from eq 14 up to the size parameter $B \sim 1$ introduced in eq 11, which apparently can be determined from the comparison of $D(t)$ and $V(t)$ provided the free volume theory is applicable to temperatures below T_g. This will be tested by our experiments presented in Figure 5.

Free volume is often considered to be a geometric quantity composed of "local free volume elements" having a well-defined size distribution. This conception is supported by experiments on photoisomerization of photochromic and fluorescent probe molecules in glassy polymers.[29] Whereas the local free volume is determined in these experiments by the "isomerization volume" of the probe molecules, our diffusion experiments refer to displacement over distances larger than 150 nm

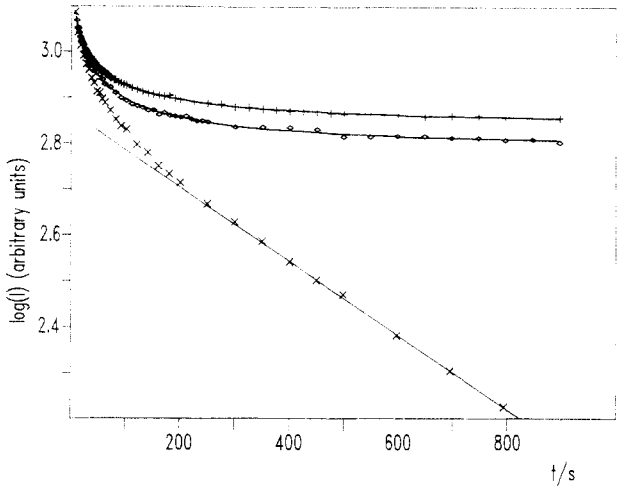

Figure 1. Initial decay of FRS intensity for TTI in poly(ethylstyrene) at 59.5 °C. The grating distances of the three runs are (from above) 25.4, 4.22, and 0.319 μm.

and will thus provide an independent test of the "geometric" interpretation of free volume. It will turn out that the assumption of a dynamic coupling between probe and matrix motion is more appropriate for interpreting our results.

II. Experimental Part

(1) Diffusion Experiments. Diffusion coefficients of photoreactive dye tracer molecules have been measured by application of a holographic grating technique where the diffusive decay of a photochemically produced grating is monitored by recording the intensity of forced Rayleigh scattering (FRS) as a function of time.[7] Our present setup[30] uses the wavelength λ = 488 nm of an Ar ion laser where the grating distance $d = \lambda/2 \sin(\theta/2)$ can be varied from ~20 μm to almost the minimum $\lambda/2n \sim 160$ nm achievable with "reflection holography" at the limiting beam crossing angle of $\theta = 180°$. For diffusion times of 2–3 days the minimum D values attained are close to 10^{-17} $cm^2 s^{-1}$ (see Figure 2), whereas our maximum values are at about 10^{-7} $cm^2 s^{-1}$. The samples have the form of pellets with 8-mm diameter and 0.3-mm thickness. The solute concentrations were kept below 0.5% in all experiments. Below this value no concentration dependence is detectable. Thus, we may confidently interpret our diffusion coefficients as identical with those of the infinitely diluted state. The samples were usually prepared by freeze-drying a benzene solution of the dye and the corresponding matrix, pressing the resulting powder into the form of a pellet, and annealing for 3–4 h in the sample holder in order to improve homogeneity and relax internal tensions. Other procedures, described in ref 31, were used in some cases, e.g., for the TNB solutions. Typical bleaching parameters are 50–200-mW laser power for 10–100 ms and a spot diameter of 0.2–1 mm. For holograms of comparable efficiency somewhat higher intensities are necessary for the ONS than for the TTI dyes described below. The FRS scattering intensity could generally be fitted by the exponential $I(t) = [A \exp(-t/\tau) + B]^2 + C$ with $\tau^{-1} = 4\pi^2 D/d^2$ and small background corrections B and C.[30] However, in polymer glasses below T_g there was an additional initial decay which is shown for the example of TTI in polyethylstyrene (PES) in Figure 1. The initial decay typically amounts to 20–40% of the total decay, can be fitted with a stretched exponential or a superposition of two exponentials, and is independent of the grid spacing d. When fitted with a stretched exponential $\exp[-(t/\tau_0)^\beta]$, τ_0 seems to increase with decreasing temperature, the apparent activation energy being below 20 kJ mol^{-1}. The width parameter β is typically between 0.3 and 0.5. The reproducibility of τ_0 and β is rather poor and may be related to bleaching conditions, the spot location in the sample, possibly, dependent upon local tensions in the glass.

(2) Photochromic Dyes. TTI. We shall use the abbreviation TTI for the tetrahydrothiophene–indigo derivative having the systematic name, 2,2′-bis(4,4-dimethylthiolan-3-one): TTI

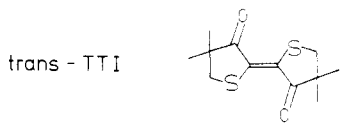

is synthesized in a three–four step procedure starting from commercially available compounds as published in the literature.[32,33] The photochemistry of this dye has been thoroughly investigated in solute and solid matrices by Baro.[34] His results show a pure photochemical cis–trans isomerization without any occurrence of side products for both directions in all matrices. Furthermore, the quantum yields and photostationary concentrations were the same in solid PMMA and in solution (which is, e.g., not the case for azobenzene or larger thioindigo derivatives) reflecting the small activation volume of TTI isomerization. No photoreaction occurred in the low-M glass-forming mixture 2-methylbutane/3-methylpentane 6:1 at 77 K—a hint for the much more efficient packing in such a van der Waals glass. The absorption maxima in PMMA of *trans*-TTI at 452 nm and *cis*-TTI at 398 nm were both about log (ϵ) = 4.0, the magnitude being 30% reduced compared to the solution value. Our FRS bleaching and reading was carried out at 488 nm, which is in the long-wavelength tail of the trans absorption and well outside of the cis absorption, so that we conclude that our holograms are of the mixed type but mainly originate from phase differences. The big distance from cis absorption may also explain the experimental fact that we never saw any hint of two diffusing species. Therefore we conclude that our diffusion coefficients are for the *trans*-TTI (or, if they are caused by both isomers, both diffusion coefficients must be of the same order of magnitude).

TTI is considered to have a very high thermal stability (no decomposition below 320 °C) in the literature,[32] the thermal isomerization from cis to trans starting at 160 °C. This is in agreement with our observation that samples of *trans*-TTI dissolved in a polymer matrix and mounted into the sample holder do not show any fading on heating above 200 °C or being kept at 150 °C for several days. However, we found (in agreement with ref 34) that prolonged heating of a solution of TTI in the presence of oxygen will irreversibly destroy the dye. In order to have an estimate when thermal contributions to the signal decay have to be taken into account, we studied the recovery after bleaching of *trans*-TTI dissolved in the styrene oligomer PS-20 (a matrix of low viscosity) by an absorption experiment using our conventional sample preparation procedure and geometry (no explicit elimination of oxygen). The time scales thus obtained are about 1000 s at 160 °C and 10 000 s at 120 °C. Such a temperature dependence is typical for isomerization of thioindigo derivatives. Diffusion experiments were usually carried out on an at least 2 orders of magnitude faster time scale; only the slowest aging runs in PC may have a contribution of a few percent originating from thermal decay.

ONS Derivatives. The *o*-nitrostilbene (ONS) system has already been applied in our investigations of polymer–polymer diffusion[35,36] and our first measurements of probe diffusion at the glass transition.[8] The synthesis[36–38] leads to the nitrile, ONS-N, which is used as the first probe. By hydrolyzing the nitrile,[36] one obtains the corresponding carboxylic acid, which is transformed into its cesium salt. The usual reaction of this key product with commercially available benzyl chloride or respectively with 4-(bromomethyl)azobenzene (synthesized in two steps using standard procedures) in carefully dried DMF yields the expected condensation products ONS-B and ONS-A. The dyes were purified by using preparative-layer chromatography on silica gel 60 (Merck)/dichloromethane. The UV–vis spectra showed the expected bands (typical absorption of ONS and azobenzene in ONS-A). ONS-B was also checked with high resolution ^1H NMR.

As the π-systems are decoupled and we illuminate the ONS part of the molecules we expect the photochemistry of this kind of ONS derivatives to be the same as has been studied previously.[38] The thermal isomerization of the azobenzene moiety in ONS-A is very quick at the interesting temperatures, so that we do not have to take it into account. The photochemical ring closure of ONS leads irreversibly to the corresponding

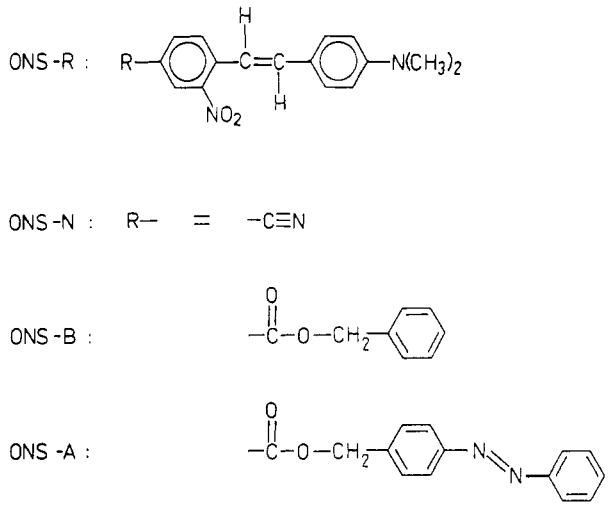

dihydroisatogene, which is oxidized under thermal control to the blue isatogene. This thermal step is much faster than diffusion above 150 °C. At 140 °C the thermal reaction is typically completed after 5 min and allows for determining the small D values of the ONS dyes in PC down to this temperature (see Figure 7). In principle, we could have separated the diffusion and the chemical reaction contributions by analyzing the FRS decay curves as a function of the grating distance. However, we preferred using the TTI probe at lower temperatures and only varied the grating distance for control purposes.

(3) Matrix Properties. Of the different matrices investigated in this study, sufficient and appropriate data for a free volume analysis[13] was found in the literature only for polystyrene (PS), bisphenol A polycarbonate (PC) and tri-α-naphthylbenzene (TNB). For the other matrices, we performed dynamic mechanical experiments and determined thermal expansion coefficients from index of refraction measurements when necessary for sample characterization.[39] A Rheometrix RMS 800 rheometer was used with plate plate geometry in an oscillating low-amplitude mode (2%) in a frequency range between 10^{-2} and 10^{2} rad s^{-1}. By the usual temperature frequency shift procedure, master curves were obtained for an appropriate reference temperature. By analysis of the shear moduli $G'(\omega)$ and $G''(\omega)$ and the temperature shift factor a_T using standard procedures,[13] the free volume parameters, α_f/B and f_g/B, listed in Table I, and the monomeric friction coefficients $\zeta_0(T_g)$ for calculating $D_{matrix}(T_g) = k_B T_g/\zeta_0(T_g)$ (Table II) were obtained. The results are briefly discussed below and summarized in the tables.

Polystyrene (PS). We used an anionically polymerized sample of M_n = 270 000 g mol^{-1} and M_w/M_n = 1.32 prepared in our own laboratory. The polydispersity was due to high molecular weight tailing in all of our anionically prepared polymer matrices (PS, PES, PMMA, PEMA). We carefully avoided the presence of oligomers or monomer impurities. The free volume parameters, α_f/B and f_g/B, were obtained from ref 40, the expansion coefficients above and below T_g, α_l and α_g, from ref 41, and the monomeric friction coefficient ζ_0 at T_g from ref 13. We have adopted the same parameters for the *styrene oligomer* PS-20, M_n = 2080 g mol^{-1}, M_w/M_n = 1.05, prepared in our laboratory, since no large M dependence is reported in the literature in this molecular weight range, except for T_g that was determined as 339 K in our DSC experiments (at 10 K min^{-1}). Mixtures of PS (M_n = 270 000 g mol) and 10 wt % *tricresyl phosphate* (PS/TCP) (mixture of the isomers, Fluka) were prepared by freeze-drying benzene solutions. Our dynamic mechanical experiments were done in a temperature range of 80–150 °C and analyzed as described above.

Thermal expansion coefficients were calculated from published index of refraction data.[31,42]

Poly(ethylstyrene) (PES). The PES, M_n = 77 000, M_w/M_n = 1.05, used in this study was prepared by anionic polymerization. Dynamic mechanical experiments were done in a temperature range of 90–150 °C.[31] Index of refraction measurements were done in a temperature range of 25–135 °C. Below T_g, the sample was cooled in steps of 5 K and n recorded after 1-h waiting time in each step. We obtained $(dn/dT) = -3.54 \times 10^{-4}$ K^{-1} for $T > T_g$ and -2.09×10^{-4} K^{-1} for $T < T_g$. The resultant[31] α_l and α_g values are given in Table I.

Poly(methyl methacrylate) (PMMA). The published dynamic mechanical data differ due to different tacticities. The PMMA, M_n = 260 000, M_w/M_n = 1.76, used in this study was prepared by anionic polymerization; the high T_g = 121 °C confirms the predominant atactic structure with a somewhat increased syndiotactic content. Dynamic mechanical experiments were done in a temperature range of 140–220 °C.

Poly(ethyl methacrylate) (PEMA). The PEMA, M_n = 110 000, M_w/M_n =1.2, used in this study was prepared by anionic polymerization. Dynamic mechanical experiments were done in a temperature range of 90–180 °C. As with PMMA, the obtained free volume parameters and the monomer friction coefficient (see Tables I and II) differ considerably from literature values,[31] since they may depend critically upon tacticity.

Bisphenol Polycarbonate (PC). A commercial sample, Macrolon (Bayer AG), was used with M_w = 35 000 g/mol and a broad M_w distribution. Free volume parameters, ζ_0, α_l, and α_g, were obtained from ref 43.

Tri-α-naphthylbenzene (TNB). The sample used in this study was obtained from J. H. Magill, Mellon Institute, Pittsburgh, PA, who has also performed a thorough study of the physical properties, which is published in ref 44 and the papers cited therein.

III. Results and Discussion

(1) Diffusion of TTI in Different Matrices. In Figure 2, the diffusion coefficients of the same probe molecule TTI in different matrices are drawn versus $1/T$ along with the free volume fit curves calculated from eqs 1–11, the fit parameters being listed in Tables I and II. The assumption (cf. eqs 3a and 6) that the Vogel temperature $T_\infty = T_g - C_{2g}$ is the same for matrix and probe mobility provides a satisfactory fit. A simultaneous fit of both WLF parameters C_{1g} and C_{2g} yields little improvement in the PS and PES samples where C_{1g} changes by less than 5% and C_{2g} by less than 10% in comparison with the fit where only C_{1g} is variable. Larger changes occur in the other matrices,[31] in particular, C_{2g} is reduced by 17, 75, and 52 K in PMMA, PEMA, and PC, respectively, and increased by 52 K in TNB. It is also possible to fit the data with an additional amount of energetic activation[45] up to about 80–100 kJ/mol without significant change of the fit curves.[31] It is apparent from Figure 2 that the experimental D values bend over from the WLF curves at some temperature T_g^{eff} (see Table II), about 4–5 K below the thermal glass temperature T_g. We believe that the differences between T_g and T_g^{eff} result from the different time scales of the DSC and diffusion experiments; the DSC scans were recorded at 10 K/min whereas about a 1-h annealing preceded the diffusion experiments. This has a particularly large effect in PC (Figure 6), where physical aging is known to be unusually fast[46] (see below). Only D values measured above T_g are included in the WLF fits discussed above. However, in determining the coupling parameters ξ and λ (see Table II) from eqs 1–3 we used T_g^{eff} in the systems where it could be determined from the diffusion measurements.

In Figure 2a, the D values are shown for diffusion in PS and three matrices where additional "free volume" was introduced in the form of additional chain ends (styrene oligomer PS-20), through a monomer additive (10% TCP) and by covalent bonding of mobile p-ethyl groups along the chain (PES). Apart from the shift in T_g, the changes are small for PS-20 and PS/TCP. A simultaneous fit of all three PS samples by eq 1 was possible and is shown in Figure 3 where log D is drawn versus T

Table II
Free Volume Analysis of Tracer Diffusion

matrix	tracer	$-\log D_{matrix}(T_g)$	$-\log D(T_g)$	$-\log D(T_g^{eff})$	T_g^{eff}/K	$-\log D'_0$	ξ	λ
PS	TTI	16.7	14.1	15.0	369	2.6	0.84	0.26
PS-20	TTI	16.7	13.9			2.9	0.80	
PS/TCP	TTI	16.8	14.1	14.9	338	2.8	0.74	0.17
PES	TTI	15.9	12.5	13.3	350	2.8	0.72	0.31
PMMA	TTI	16.3	14.0			5.0	0.69	
PEMA	TTI	17.1	14.2			1.7	0.81	
TNB	TTI	18.1	15.1			-7.7	0.81	
PC	TTI	16.3	11.2	13.2	412	3.1	0.50	0.29
PC	ONS-N	16.3	12.0			2.3	0.60	
PC	ONS-B	16.3	12.0			2.5	0.59	
PC	ONS-A	16.3	13.5			0.9	0.77	

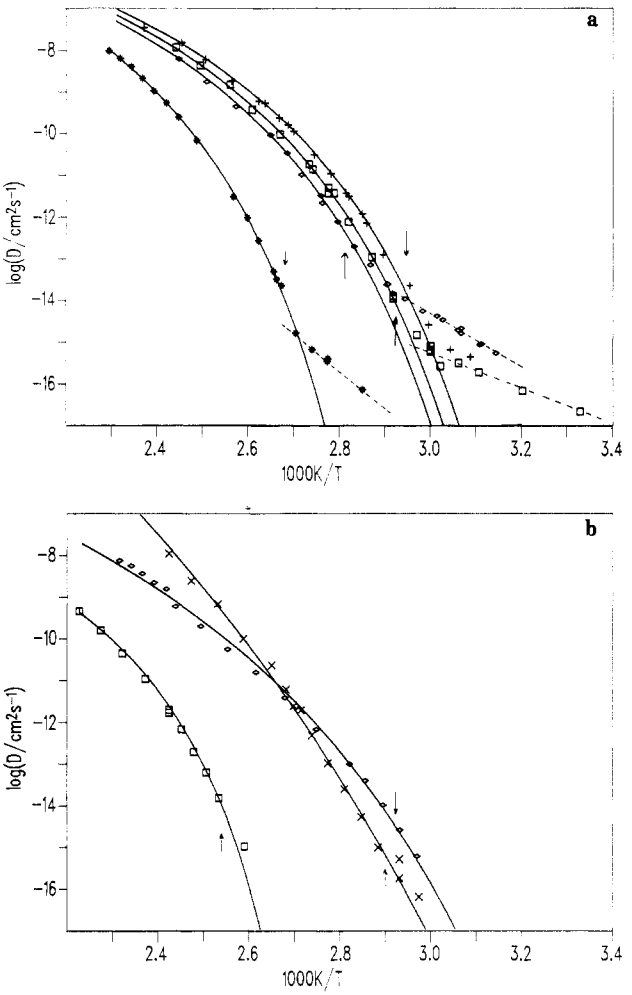

Figure 2. Diffusion coefficients D of TTI in different matrices, drawn versus $1/T$. (See Table I for abbreviations.) (a, Top) (PS) (*); PS-20 (+); PS/TCP (□); PES (◇). (b, Bottom) PMMA (□); PEMA (◇); TNB (×). (The arrows indicate T_g.)

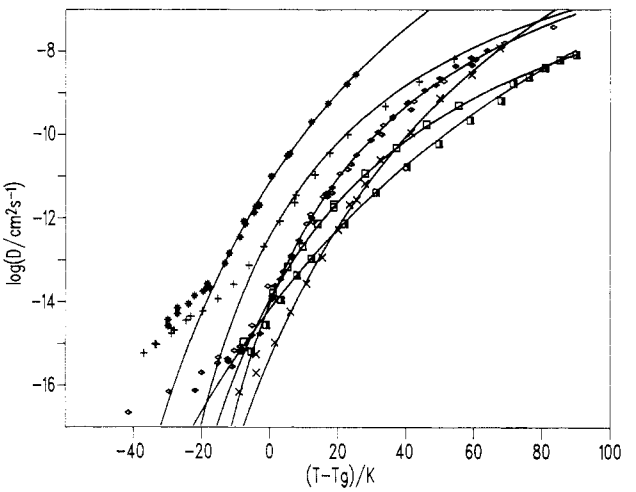

Figure 3. Diffusion coefficients D of TTI in different matrices, drawn versus $T - T_g$: PS (◆); PS-20 (◇); PS/TCP (◪); PES (+); PMMA (□); PEMA (◨), TNB (×).

$- T_g$. The PES curve is considerably above the PS curve in Figure 3, indicating that the mobile ethyl groups allow for much higher probe mobility though the T_g shift is comparable to that of the other "modified" polystyrenes. Whereas the fit by eqs 1–3 in still satisfactory for PMMA, deviations well outside our experimental accuracy are seen in Figure 2b for PEMA and TNB. As mentioned above, the fits can be improved by allowing for variation of C_{2g} or some activation energy. The latter may be justified in PEMA due to some influence of side group motion (β-processes) above T_g. It is remarkable that $D(T_g)$ in both methacrylates is not larger than in PS. The lowest $D(T_g)$ is observed in the monomer glass TNB, and a further reduction by almost two decades is found in *o*-terphenyl.[47] This demonstrates the larger coupling of probe diffusion to the α-process in monomer glasses where the sizes of probe and matrix molecules are of the same order. Surprisingly, the ξ parameter of TNB is not larger than in the polymer glasses. However, we should note (see Table II) the huge value of the preexponential factor D_0' of TNB, which originates from the very small value of the fractional free volume f_g at T_g (see Table I) since

$$\log D_0' = \log D(T_g) + \xi B/(f_g \ln 10) \qquad (16)$$

as can be derived from eqs 4–11. It is also apparent from Figures 2b and 3 that the temperature dependence of TNB differs qualitatively from that in all polymer glasses. Organic van der Waals glasses as TNB and *o*-terphenyl (also termed "fragile"[48]) are known to be better approximated by the Arrhenius law at temperatures close to T_g.[44,49]

In four systems it was possible to measure TTI diffusion in the glass below T_g. The samples were annealed for several hours at the lowest temperature and the measurements done at successive increased temperatures (see below for aging effects). In the styrene oligomer (PS-20) and TNB, crack formation impeded diffusion experiments well below T_g. The fit by eqs 1 and 3b with T_g^{eff} as reference yield the λ parameters listed in Table II. An Arrhenius equation fits the data equally well with apparent activation energies of 170, 90, 120, and 220 kJ/mol for PS, PS/TCP, PES, and PC, respectively.[31] The small temperature range available to us below T_g and the uncertainly about possible aging effects render impossible any decision whether the Vrentas–Duda or the Arrhenius fit is more appropriate. However, the value of $\lambda = 0.26$ given in Table II for PS is comparable to other values reported previously ($\lambda = 0.20$–0.24) and below the upper bound value of 0.30 given in ref 50.

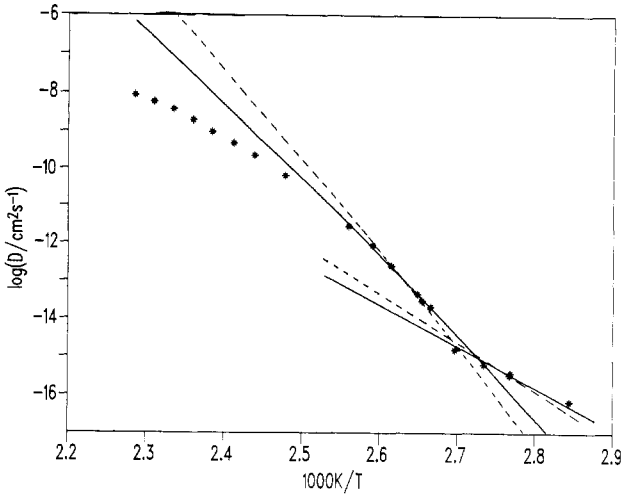

Figure 4. Comparison of TTI diffusion in PS with a T^2 law, eq 13 (see text).

In Figure 4, we have compared TTI diffusion in PS with the T^2 law, eq 12, proposed by Bässler et al.[22,23] The full lines were obtained by fitting the six D values measured at 375–390 K to eq 13 and assuming an Arrhenius law with the apparent activation energy $k_B T_0^2/T_g$ to be valid at $T < T_g$.[22,23] The dashed lines were obtained by fitting the six D values between 370 and 386 K. The fit parameters are (dashed line in brackets) T_0 = 3020 K (3300 K), log D_∞ = 14.6 (19.8), and T_g = 367 K (371 K). Thus, the fit is rather sensitive to the choice of the temperature range used for the fit, and the experimental data fall below the T^2 line at temperatures above $\sim T_g$ + 15 K. It should be noted that the T^2 lines are hardly different from the Arrhenius law in the T range considered. Thus, we conclude that probe diffusion in polymer glasses is much better described by the WLF equation than by the T^2 law. Nevertheless, the relaxation model of Bässler et al. has very attractive features, in particular, no additional fit parameter is necessary in order to estimate the apparent activation energy below T_g. It is also apparent from Figure 2b that diffusion in TNB (and *o*-terphenyl[47]) can be fitted to a T^2 law over a larger temperature range. However, in polymer glasses, the model should be modified, perhaps, by assuming a non-Gaussian distribution of energy barriers.[51]

(2) Physical Aging. At temperatures below T_g the measured D values become a function of the annealing time. This effect of physical aging can be expected from our considerations in the Introduction since the time dependence of the fractional free volume $f(t)$, which is assumed to cause volume retardation, eq 14, also influences the diffusion coefficient through eq 15. The determination of D is problematic if it varies substantially with aging during the time of measurement. Therefore, we have annealed the samples for a minimum time of 10^3 s after quenching from T_g + 20 K to the temperature of measurement. The horizontal error bars in Figure 5a indicate the measuring period; the vertical bars are our error estimates of D at the location t. We have plotted in a log–log plot the ratio of $D(t)$ to its equilibrium value $D(\infty)$ as extrapolated from our D measurements above T_g through eq 4. The results for TTI diffusion in PS, PES, and PC at various temperatures below T_g are shown in Figure 5a. In PC, the value of $D(t)$ approaches $D(\infty)$ within a few hours at temperatures within T_g and T_g – 20 K (see Figure 3). Accordingly, we had to study physical aging at lower temperatures, where $D(t)$ appears to follow a power law $D(t) = At^{-\alpha}$ with α = 0.24 ± 0.04 and

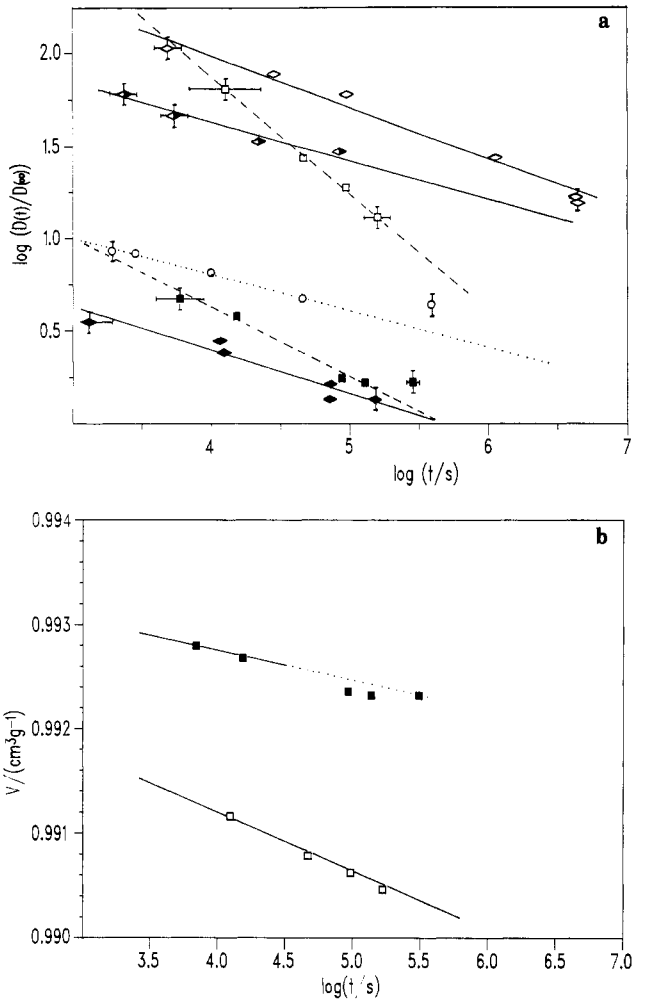

Figure 5. Physical aging in polymer glasses. (a, Top) Ratio D over the extrapolated equilibrium value $D(\infty)$, drawn versus aging time in a log–log plot. PS: 92 °C (■); 88 °C (□). PES: 72 °C (○). PC: 132 °C (◆), 123 °C (◪); 120 °C (◇). (b, Bottom) Specific volume of PS at 92 °C (below) and 88 °C (above). The full and dotted lines are from volume retardation experiments of Hozumi;[54] and the squares are calculated from eqs 14 and 15 (see text).

a temperature-dependent prefactor A. The adjacent experimental points at 131.5 °C and log t = 4.85 were measured at different spots of the sample. The difference is possibly due to local heterogeneities, which cause cracks in oligomer and monomer glasses. Better reproducibility was obtained in runs where all D values were measured at the same spot. The origin of the fast aging in PC may be related with the internal main chain mobility.[46,52] In PES, the experimental D values seem to approach a limiting value $D(\infty)$ well above the WLF extrapolation. This may be a consequence of the ethyl group mobility (β-process) in PES glass. Perhaps the same occurs in PS (at 92 °C) to a lesser extent; however, the uncertainties of the experiment and of the WLF extrapolation are also within a factor of ~2.

We have attempted to compute volume retardation from $D(t)$ in PS at two temperatures as explained in the Introduction. The result is shown in Figure 5b where the lines are the specific volumes determined by interpolation from the volume retardation data of Hozumi.[53,54] The squares were obtained from the $D(t)$ values shown in Figure 5a and Hozumi's[54] limiting values $V(\infty)$ by application of eqs 14 and 15. Since the thermal expansion coefficient 5.4×10^{-4} K^{-1} of $V(\infty)$ as obtained from ref 54 is within the α_1 values published[41] for PS at $T > T_g$ (see Table I),

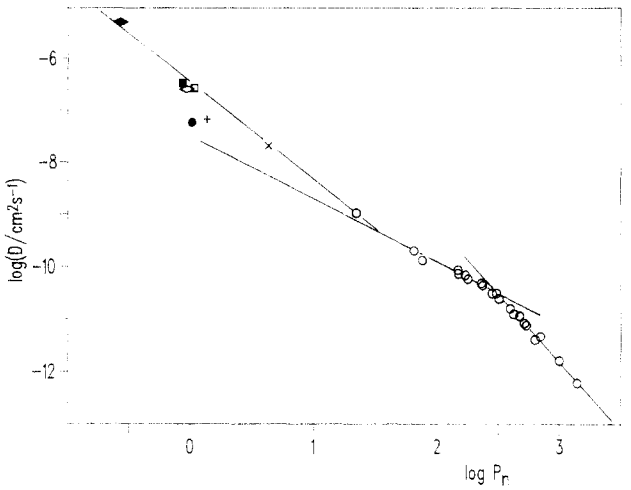

Figure 6. Diffusion coefficents D of different solutes in PS at 185 °C, drawn versus a ficticious degree of polymerization P_n defined in the text. The straight lines indicate the entangled, Rouse, and incomplete coupling ($\xi < 1$) regimes. Methane (◆); benzene (■); toluene (◇); ethylbenzene (□); camphorquinone (●); TTI (+); ONS-A (×); p-nitroaniline (▼); p-aminoazobenzene (▲); yellow 7 (▲); PS-ONS (○).

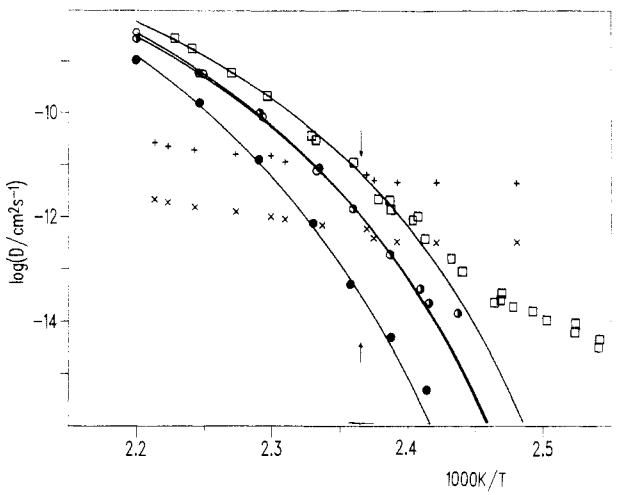

Figure 7. Diffusion coefficients D of different solutes in PC (the arrow indicates T_g): TTI (□); ONS-N (○); ONS-B (◑); ONS-A (●). See text for values of CQ (+) and its photoproduct (×).

only $V(\infty)$ at one temperature below or even above T_g is necessary. The agreement of the computed and measured volumes is quite remarkable. It is probably the first direct experimental relation of a transport variable with volume retardation below T_g, and it certainly confirms the free volume concept. The only fit parameter in relating $D(T)$ and $V(T)$ through eqs 14 and 15 is the size parameter B introduced in eq 11. We obtain B = 0.48, which is rather close to the values $0.53 \lesssim B \lesssim 0.77$ obtained by comparing α_f/B obtained from the WLF equation with $\alpha_f = \alpha_l - \alpha_g$ where α_l and α_g are thermal expansion coefficients published for PS above and below T_g, respectively.[41] (The numbers given in Table I yield B = 0.66.)

(3) Diffusion of Different Tracers in the Same Polymer Matrix. The dependence of tracer diffusion coefficients upon the size of the tracers has been investigated previously in polymer matrices.[1-6,13] Our goal was to bridge the gap between monomer, oligomer, and polymer diffusion in the same polymer matrix. One should expect that the coupling parameter ξ increases on increasing the probe size and approaches the limit $\xi = 1$ at some oligomer size where the Rouse model of polymer diffusion becomes applicable. Possibly, the crossover from $\xi < 1$ to $\xi = 1$ can be related with the size of "cooperatively rearranging regions" introduced in the theory of relaxation in glass-forming liquids.[16] Ideally, one should prepare a full series of labeled oligomers, say, from ethylbenzene up to labeled PS, and investigate their diffusion in a PS matrix in order to determine the crossover, possibly, as a function of temperature. The results shown in Figure 6 are a first attempt in this direction. We have defined a "ficticious" degree of polymerization P_n as the ratio of the largest diameter of the respective probe molecule (determined from molecular models using the known bond lengths and angles) to that of ethylbenzene, which was normalized to $P_n = 1$. The D values of methane,[55] benzene, toluene, ethylbenzene,[56] and p-nitroaniline, p-aminoazobenzene, and the disperse dye yellow 7[4] are literature values (obtained from inverse gas chromatography or from desorption experiments[4]) interpolated to 185 °C. All other D values are from FRS experiments: camphorquinone (CQ) by extrapolation from a WLF fit of the data of Zhang et al.,[57,58] TTI, ONS-A, and PS-23 oligomer from the present work, and the other PS data from our previous measurements at 185 °C.[59] The straight lines in Figure 6 represent an attempt to determine the crossovers between the entangled and Rouse regimes ($P_n \approx 300$) and the regimes of full ($\xi = 1$) and incomplete ($\xi < 1$) coupling ($P_n \approx 40$), respectively. Though the crossover value of $P_n = 40$ is rather crude, we have estimated the size of cooperative regions by assuming[41] $R_0/\text{nm} = 0.0685M^{1/2}$ for the relation between the end-to-end distance R_0 and the molecular weight M which results in a size of 4.4 nm, rather close to an estimation of ~3–4 nm proposed by Donth,[60] however, at the glass transition. The different D values shown in Figure 6 around $P_n = 1$ may be due to the uncertainty of the WLF extrapolation (by 58 K for CQ and 20 K for TTI) of the values determined by FRS, however, different coupling parameters ξ for different probe molecules of the same size are also possible due to different interactions with the matrix. Thus the slope determined as 1.8 in the $\xi < 1$ regimes is not expected to be a universal property, though it should always be larger than the slope 1 of a pure Rouse regime. Only in the high-temperature limit far above T_g, in the Stokes–Einstein range where the validity of WLF begins to fail, we would expect slope 1 for dyes and oligomers.

In Figure 7 the D values of some probe molecules of different size in a PC matrix are shown as a function of $1/T$. We also show literature values obtained for camphorquinone and its photoproduct by simultaneous analysis of the FRS decay caused by the diffusion of both probes.[61] The extremely small temperature dependence results in diffusion coefficients that are *smaller* by several decades than those of our largest probes at high temperatures. Since this unusual behavior may be due to an artifact of the analysis, we omit the data from our further discussion.[62] The other D values decrease with increasing probe size and can be fitted by eq 4 where the fit parameters ξ and D_0' both increase with increasing probe size (see Table II). However, there seems to be no simple relation of ξ with the solute volume (see below).[16-18] In particular, D is almost the same for ONS-N and ONS-B though the nitrile and benzyl groups are rather different in size. Perhaps the internal flexibility of the benzyl group causes an increased mobility.

We have also tried to relate the solute diffusion coefficients with the matrix viscosity η by the Stokes–Einstein relation $D = k_B T/\eta f(r)$ where $f(r)$ should only depend

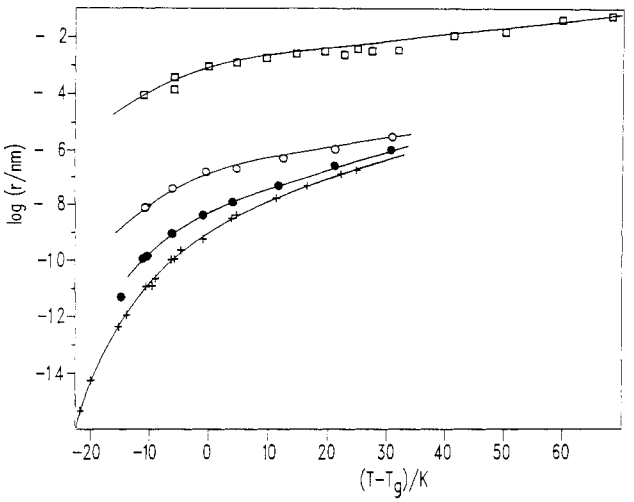

Figure 8. Stokes radii as defined in the text, drawn versus $T - T_g$: TTI in TNB (□) and TTI (+), ONS-B (●), and ONS-A (○) in PC.

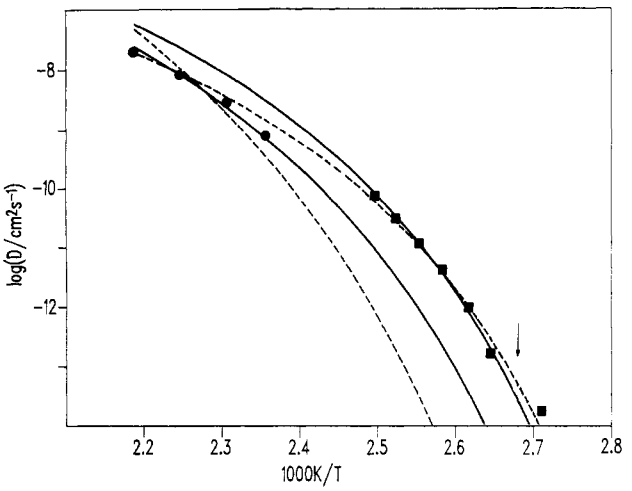

Figure 9. Comparison of ONS-A (●) and camphorquinone (■) diffusion in PS with modified WLF curves calculated from eq 18 (dashed lines) and eq 19 (full lines).

upon the size and shape of the solute ($6\pi r$ for spheres). Since $f(r)$ is usually found smaller than predicted from solute size in liquids, one has introduced a local "microviscosity"[63] η_{loc} or other concepts[64] in order to account for this effect. Whereas in normal liquids η_{loc} is found proportinal to η, this assumption results in a temperature dependent solute size as the glass transition is approached (see Figure 8), which is certainly untenable on physical grounds. The ficticious solute radii shown in Figure 8 are calculated from the Stokes–Einstein relation and literature values of the matrix viscosity. In TNB, the TTI radius approaches a value of ~0.1 nm at temperatures far above T_g, which is typical for diffusion in normal liquids. The extremely small radii in PC originate partly from the length of the polymer chains. Thus a more localized "monomeric" viscosity defined as the ratio of the polymer viscosity over the degree of polymerization, $\eta/140$, appears more appropriate, though the resulting radii shifted upward by log 140 in Figure 8 will still be below the TNB curve. It should be noted that the ratio of the ONS-B and TTI radii remains constant over a sizeable temperature range in Figure 8, its value of ~2 being on the order of the ratio of the molecule sizes. However, the large T dependence of the ficticious radii clearly demonstrates that the factorization of the solute friction parameter ζ into some microviscosity and a factor depending only upon the solute size is not possible. There is another way of looking at the "microviscosity" defined through $D = k_B T/\eta_{mic} f(r)$. If we rewrite eq 1 and 2 for $T \geq T_g$ as $\log a_T(\text{solute}) = \xi \log a_T(\text{matrix})$, it is readily seen that η_{mic} is proportional to η^{ξ} where ξ depends upon solute and matrix proporties as is shown in more detail below.

(4) Coupling of Tracer and Matrix Mobility. As we have mentioned in the Introduction (eq 3), Vrentas and Duda[3,5,6,16-19] have interpreted ξ as the ratio of the critical molar volumes of the solute and polymer matrix jumping units, $\xi = V_s^*/V_m^*$. Furthermore, they have shown[3,5] that a linear relation holds between $\xi C_{1g} C_{2g}$ and the solute molar volume V_0 at 0 K for the diffusion of a large number of solutes in PS at temperatures above T_g. V_0 was calculated from literature data[69] and assumed to be proportional to V_s^* provided the solute molecule moves as a single unit. More flexible solutes that "move in a segmentwise manner" fall considerably below the linear relationship since the molar volumes of their jumping units are lower than the molar volumes of the entire solute molecule.[5,6] Thus, the interpretation of ξ by Vrentas and Duda can only be applied easily to rigid solute molecules. Furthermore, while they have tested their interpretation for many solutes in the same matrix, little has been done for comparing ξ for the same solute in different matrices.

In Figure 9, we show the results of a test of whether ξ can be interpreted as a ratio

$$\xi_m^{\,s} = V'_s/V'_m \tag{17}$$

of some molar volumes V'_s and V'_m, which are pure solute and matrix properties, respectively, but otherwise unspecified. We have determined experimentally the ξ values $\xi_{m1}^{\,s1}$, $\xi_{m1}^{\,s2}$, and $\xi_{m2}^{\,s2}$ for the solutes s1 = ONS-A and s2 = TTI and the matrices m1 = PC and m2 = PS and have calculated the fourth ξ value from eq 18 as

$$\xi_{m2}^{\,s1} = (\xi_{m1}^{\,s1}/\xi_{m1}^{\,s2})\xi_{m2}^{\,s2} \tag{18}$$

The WLF curve, eq 4 for this calculated $\xi_{m2}^{\,s1}$ is the dashed line on the left of Figure 9. Expectedly, it provides a bad fit of the four measured D values of ONS-A in PS since ONS-A is rather flexible and should move in a "segmentwise manner". In the second example, we have chosen s1 = CQ (camphorquinone), s2 = TTI, m1 = PMMA, and m2 = PS where we have used CQ data of Zhang et al.[9,12,58] and our TTI data for determining the orther three ξ values. The WLF curve from the calculated $\xi_{m2}^{\,s1}$ (dashed line on the right of Figure 9) provides a fair fit of the experimental D values for CQ in PS. This is not surprising since CQ and TTI are rather rigid molecules, and the Vrentas–Duda interpretation should be applicable. However, the curve crosses the curve of ONS-A diffusion coefficients in PS at higher temperatures, which appears unreasonable because of the big size difference of CQ and ONS-A. An almost perfect fit was obtained by the full lines in Figure 9, where $\xi_{m2}^{\,s1}$ was calculated from

$$1 - \xi_{m2}^{\,s1} = \frac{1 - \xi_{m1}^{\,s1}}{1 - \xi_{m1}^{\,s2}}(1 - \xi_{m2}^{\,s2}) \tag{19}$$

which differs from eq 18 by replacing ξ with $1 - \xi$. It is very remarkable that this equation provides a very good fit even for the combination of the rigid CQ and the flexible large ONS-A molecules in the rather different matrices PS and PC (note the main-chain flexibility in PC[52]). Thus, we feel justified to analyze eq 19 in more detail.

Table III
Ratios of Decoupling Parameters As Defined in the Text

solutes (k)	benzene	toluene	CQ	TTI	ONS-N	ONS-B	ONS-A	polymer
R_m^{s1k}	0.25	0.48	0.7/0.65	≡1	1.25	1.22	2.17	∞
matrices (b)	PS	TNB	PEMA	oligo S	PS/TCP	PES	PMMA	PC
R_{m1b}^{s}	≡1	0.84	0.84	0.8	0.62	0.57	0.52	0.32

By rewriting it as

$$R_m^{sjk} = \frac{1-\xi_{m1}^{sj}}{1-\xi_{m1}^{sk}} = \frac{1-\xi_{m2}^{sj}}{1-\xi_{m2}^{sk}} \quad (j, k = 1, 2) \qquad (20)$$

we find that the ratio R_m^{sjk} for any pair of solutes j and k determined in the same matrix should be a pure solute property, invariant with changes in the matrix. Furthermore, we can rewrite eq 19 as

$$R_{mab}^{s} = \frac{1-\xi_{ma}^{s1}}{1-\xi_{ma}^{s1}} = \frac{1-\xi_{mb}^{s2}}{1-\xi_{mb}^{s2}} \quad (a, b = 1, 2) \qquad (21)$$

thus finding the ratio R_{mab}^{s} for any pair of matrices a and b should be a pure matrix property, invariant with changes in the solute. In Table III, we have listed the ratio R_m^{s1k} for some solutes k using TTI as a reference ($j = 1$), which should be valid for any matrix, and the ratios R_{m1b}^{s} for some matrices b using PS as a reference ($a = 1$), which should hold for any solute. Although, the validity of the numbers given in Table III is yet to be substantiated by doing more extensive experimental tests, the quality of the fits shown in Figure 9 appears rather encouraging.

So far, we have treated eq 19 as a purely phenomenological relation. The physical background may become apparent as we assume that ξ has an upper limiting value of $\xi_m = 1$. Since solute diffusion now follows the WLF equation of the matrix motion it may be termed the limit of maximum coupling.[15,69] This is also in harmony with our interpretation of Figure 6 discussed above. Now eq 19 can be interpreted in terms of a *decoupling* parameter, $\xi_m - \xi = 1 - \xi$, which accounts for the decoupling of solute diffusion from the matrix motion. The nature of this decoupling is still open to speculation; however, it appears plausible that the invariance properties given by eqs 20 and 21 must relate to nontrivial solute matrix interactions, and it is by no means obvious whether the free volume theory will provide the best physical explanation. One might speculate whether the Adam–Gibbs equation, eq 12, with A replaced by ξA will prove more appropriate for describing the decoupling in the case of very large or flexible solute molecules where cooperativity of solute and matrix motion becomes most important. At present, we are unable to provide a good physical picture that is as simple as the geometric free volume interpretation and also applies to flexible solutes.

It seems crucial to the understanding of eq 19 that $\xi \leq 1$. We know of one case where the authors claim to have determined a value of $\xi > 1$ outside their experimental uncertainty, namely, the diffusion of triisopropylbenzene (TIP) in PS, where $\xi = 1.3$ has been found.[5] However, from our inspection of the experimental data given in Figure 1 of ref 5 we believe[71] that more extensive experiments are necessary in order to substantiate this value, which implies that $D = 10^{-18}$ cm^2 s^{-1} at T_g. This is four decades below the $D(T_g)$ value of TTI in PS, and it should be noted that TTI is a rather rigid molecule of similar size as TIP and has a similar D value at 175 °C (see Table II and Figure 3).

We have already noted in the discussion of eq 16 that D'_0 of eq 4 depends upon the coupling between solute and matrix (see Table II). However, D'_0 can easily be eliminated by normalizing all D values to the value of $D(T_g)$ as is done in the WLF equation, eq 1. This has been done in Figure 10 where the shift parameter a_T defined in eq 1 is compared with the corresponding a_T values of other relaxation experiments. The curves clearly demonstrate the various degrees of solute matrix coupling, where dynamic relaxation of the matrix defines the α-process ($\xi = 1$). Generally, the large organic molecules used as photochromic dye tracers are much less decoupled from the α-process than the small molecules toluene and benzene, the latter falling even below the line of the β-process. At temperatures below T_g, the slope of the β-process is probably always smaller than that for diffusion of larger dye molecules, whereas smaller apparent activation energies are found for diffusion of small gas molecules.[1,2] Thus we see that the whole range of increasing cooperativity as we cross over from the β- to the α-relaxation can be studied by using probe molecules of different sizes.

Finally, let us come back to the preexponential factor D'_0 of eq 4 and the corresponding coupling parameter δ introduced in eq 7, which implies the existence of fully coupled probe molecules following a VFT equation with unprimed constants D_0 and B_0. This is questionable even for self-diffusion in monomer glasses since our rough estimates of $D(T_g)$ obtained in the Introduction from local relaxation times and from shear viscosity differed by more than two decades, indicating that cooperativity at T_g influences different dynamic variables rather differently. If we estimate D_0 from eq 16 by letting $\xi = 1$ and $D(T_g) = D_{matrix}(T_g) = k_B T_g/\zeta_0$ with monomer friction constants determined from dynamic mechanical relaxation,[13] we obtain, e.g., log D_0 values of −0.2 and −3.0 for PC and PS, respectively, to be compared with the log D'_0 values given for $\xi < 1$ in Table II. Whereas in PC there is a monotonous increase of D'_0 with increasing ξ up to D_0 at $\xi = 1$, no clear relation of ξ and D'_0 seems to exist in the other matrices, although log $D_g = -9.8\xi - 6.3$ provides a fair fit of our data,[31] which also has a plausible limiting value at $\xi = 0$ (see ref 1). From eq 4, D'_0 should be the solute diffusion coefficient in the limit $T \to \infty$. However, eq 4 is not valid at temperatures far above T_g, since our discussion of the ficticious Stokes radii shown in Figure 8 indicates that solute diffusion in normal liquids is much less decoupled from solvent mobility than in the vicinity of the glass transition.

IV. Conclusions

We have shown that the free volume description of solute diffusion in polymer matrices[13,15–19] is applicable to rather different solute sizes and polymers. The free volume parameters C_{1g} and C_{2g} defined in the WLF equation (eqs 1–3) can be adopted from mechanical relaxation of the pure matrix. The Vogel temperature $T_\infty \equiv T_g - C_{2g}$ stays essentially the same for solute diffusion whereas C_{1g} is replaced by $C'_{1g} = \xi C_{1g}$ thus defining a coupling parameter ξ, which increases with increased coupling of solute and matrix motion. Whereas the interpretation of ξ as the ratio of critical molar volumes of solute and polymer matrix jumping units is only possible for relatively small and rigid solute molecules, we find that the *decoupling parameter* $1 - \xi$ exhibits remark-

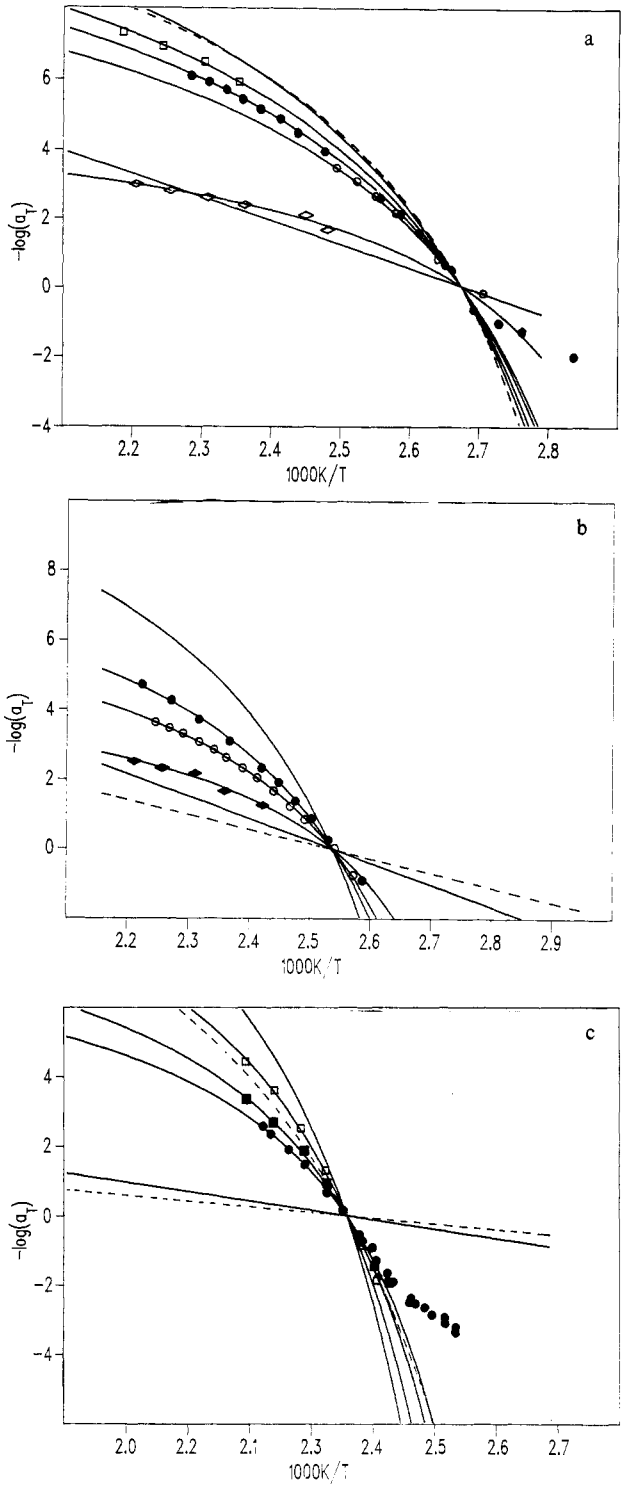

Figure 10. WLF shift parameter a_T (see eq 1) drawn versus $1/T$. The full lines without experimental points are from mechanical relaxation for the α-process (above) and the β-process. (a) PS matrix: ONS-A (□); TTI (●); camphorquinone[9,12,58] (○); benzene[56] (◇); and ONS labeled PS[59,65] (- - -). (b) PMMA matrix: TTI (●); camphorquinone[9] (○); toluene[66] (◆); dielectric relaxation[67] (- - -). (c) PC matrix: ONS-A (□); ONS-B (■); TTI (●). Dashed lines are for dielectric relaxation[68] of the α-process (above) and the β-process (below).

able invariance properties: The ratio $(1 - \xi_m^{s1})/(1 - \xi_m^{s2})$ determined for two solutes 1 and 2 in the same matrix appears to be independent of the nature of the matrix as shown for two examples in Figure 9. Furthermore, we show by rewriting eq 19 that the ratio $(1 - \xi_{m1}^{s})/(1 - \xi_{m2}^{s})$ determined for two matrices 1 and 2 is independent of the nature of the solvent, irrespective of whether the solute molecules are rigid or flexible. We have tested the effect of introducing additional "free volume" by comparing TTI diffusion in PS with that in a styrene oligomer and a plasticized PS, both having about the same T_g (66 and 69 °C, respectively). The resultant D values could be fitted by the same WLF curve as the PS data when drawn versus $T - T_g$ (Figure 3). The D values at T_g are considerably larger in PES and PC where side-group and main-chain motions (β-process) persist in the glass. $D(T_g)$ was found lowest in the monomer glass TNB, however, still much larger than expected from shear viscosity by application of the Stokes–Einstein relation. We demonstrate in Figure 8 that even the conception of local "microviscosity" cannot account for the temperature dependence of D when approaching T_g. Equations 1 and 2 imply that the microviscosity η_{mic} is proportional to η^{ξ} where ξ depends upon solute and matrix properties.

At temperatures below T_g, the D values can be described by introducing a further fit parameter in the WLF equation: $C'_{2g} = C_{2g}/\lambda$. However, an Arrhenius fit is also possible and we cannot decide from our limited data which approch is more appropriate. A relaxation model proposed by Bässler et al.[22,23] yields a fair estimate of the change in slope of $D(T)$ from above to below T_g (Figure 4), however, the D values above T_g + 20 K in polymer melts cannot be fitted by this model. Physical aging of D could be quantitatively related with volume retardation of the matrix (Figure 5). The resultant size parameter B defined in eq 11 was found of the same order as the values obtained by comparing α_f/B, determined from mechanical relaxation, with the difference of the thermal expansion coefficients, $\alpha_l - \alpha_g$, above and below T_g (see eqs 9–11). In summary, solute diffusion in polymer glasses can be described within the free volume picture above and below T_g; however, the solute matrix coupling cannot be understood in a purely geometrical sense.

Acknowledgment. We thank Professor J. H. Magill for supplying a sample of tri-α-naphthylbenzene and Dr. J. Baro who has suggested the use of TTI as a photoreactive dye and has supplied a first sample. We are indebted to Professor H. Bässler and Dr. R. Richert for fruitful discussions about their relaxation model. Support by the Deutsche Forschungsgemeinschaft is gratefully acknowledged. We thank one of the referees for pointing out to us the significance of refs 5 and 6, which we had overlooked.

References and Notes

(1) Crank, J.; Park, G. S. *Diffusion in Polymers*; Academic Press: London, 1968.
(2) Stannett, V. T.; Koros, W. J.; Paul, D. R.; Londsdale, H. K.; Baker, R. W. *Adv. Polym. Sci.* **1979**, *32*, 69 and references therein.
(3) Vrentas, J. S.; Duda, J. L. *J. Appl. Polym. Sci.* **1971**, *21*, 1215.
(4) Masuko, I.; Sato, M.; Karasawa, M. *J. Appl. Polym. Sci.* **1978**, *22*, 1431.
(5) Vrentas, J. S.; Liu, H. T.; Duda, J. L. *J. Appl. Polym. Sci.* **1980**, *25*, 1293.
(6) Vrentas, J. S.; Duda, J. L.; Hou, A. C. *J. Appl. Polym. Sci.* **1986**, *31*, 139.
(7) Eichler, H. J.; Günther, P.; Pohl, D. W. *Laser-Induced Dynamic Gratings*; Springer: Berlin, 1986.
(8) Coutandin, J.; Ehlich, D.; Sillescu, H.; Wang, C. H. *Macromolecules* **1985**, *18*, 587.
(9) Zhang, J.; Wang, C. H.; Ehlich, D. *Macromolecules* **1986**, *19*, 1390.
(10) Zhang, J.; Wang, C. H. *Macromolecules* **1987**, *20*, 683.
(11) Zhang, J.; Wang, C. H. *Macromolecules* **1987**, *20*, 2296.
(12) Zhang, J.; Wang, C. H. *Macromolecules* **1988**, *21*, 1811.
(13) Ferry, J. D. *Viscoelastic Properties of Polymers*, 3rd ed.; Wiley: New York, 1980.
(14) Angell, C. A. *J. Non-Cryst. Solids* **1985**, *73*, 1.
(15) Fujita, H. *Fortschr. Hochpol. Forsch.* **1961**, *3*, 1.

(16) Vrentas, J. S.; Liu, H. T.; Duda, J. L. *J. Appl. Polym. Sci.* **1980**, *25*, 1297.
(17) Vrentas, J. S.; Duda, J. L.; Ling, H.-C. *J. Polym. Sci. Phys.* **1985**, *23*, 275.
(18) Vrentas, J. S.; Duda, J. L.; Ling, H.-C.; Hou, A. C. *J. Polym. Sci. Phys.* **1985**, *23*, 289.
(19) Vrentas, J. S.; Duda, J. L.; Hou, A. C. *J. Polym. Sci. Phys.* **1985**, *23*, 2469.
(20) Grest, G. S.; Cohen, M. H. *Adv. Chem. Phys.* **1981**, *18*, 455.
(21) Adam, G.; Gibbs, J. H. *J. Chem. Phys.* **1965**, *43*, 139.
(22) Bässler, H. *Phys. Rev. Lett.* **1987**, *58*, 767.
(23) Richert, R.; Bässler, H. *J. Chem. Phys.*, in press.
(24) Grünewald, M.; Pohlmann, B.; Movaghar, B.; Würz, D. *Philos. Magn. B* **1984**, *49*, 341.
(25) Wagner, K. W. *Ann. Phys.* (*4*) **1913**, *40*, 817.
(26) Anderson, J. E.; Ullman, R. *J. Chem. Phys.* **1967**, *47*, 2178.
(27) Tweer, H.; Simmons, J. H.; Macedo, P. B. *J. Chem. Phys.* **1971**, *54*, 1952.
(28) Struik, L. C. E. *Physical Aging in Amorphous Polymers and other Materials*, 2nd impr.; Elsevier: Amsterdam, 1980.
(29) Victor, J. G.; Torkelson, J. M. *Macromolecules* **1987**, *20*, 2241, 2951; **1988**, *21*, 3490 and references therein.
(30) Sillescu, H.; Ehlich, D. In *Application of Lasers in Polymer Science and Technology*; Fouassier, J. P., Rabek, J. F., Eds.; CRC Press: Boca Raton, FL, in press.
(31) Ehlich, D. Dissertation, Universität Mainz, 1989.
(32) Herrmann, H.; Lüttke, W. *Chem. Ber.* **1968**, *101*, 1708, 1715.
(33) Acheson, R. M.; Barltrop, J. A.; Hichens, M.; Hichens, R. E. *J. Chem. Soc., London* **1961**, 650.
(34) Baro, J. Dissertation, Universität Göttingen, 1987.
(35) Antonietti, M.; Sillescu, H. *Macromolecules* **1985**, *18*, 1162.
(36) Antonietti, M.; Coutantin, J.; Ehlich, D.; Sillescu, H. In *Physical Optics of Dynamic Phenomena and Processes in Macromolecular Systems*; Sedlacek, B., Ed.; de Gruyter: Berlin, 1985; p 191.
(37) Pfeiffer, P. *Chem. Ber.* **1915**, *48*, 1777, 1808.
(38) Splitter, J. S.; Calvin, M. *J. Org. Chem.* **1955**, *20*, 1086.
(39) The measurements were performed at the Max-Planck-Institut für Polymerforschung, Mainz. We are grateful to Dr. T. Pakula and L. Stenner for advice and assistance.
(40) McKenna, G. B.; Hadziioannou, G.; Lutz, P.; Hild, G.; Strazielle, C.; Straupe, C.; Rempp, P.; Kovacs, A. J. *Macromolecules* **1987**, *20*, 498.
(41) Brandrup, J.; Immergut, E. H. *Polymer Handbook*, 2nd ed.; Wiley: New York, 1975.
(42) Jenckel, E.; Heusch, R. *Kolloid Z.* **1953**, *130*, 89.
(43) Mercier, J. P.; Aklonis, J. J.; Litt, M.; Tobolsky, A. V. *J. Appl. Polym. Sci.* **1965**, *9*, 447.
(44) Plazek, D. J.; Magill, J. H. *J. Chem. Phys.* **1968**, *49*, 3678.
(45) Macedo, P. B.; Litovitz, T. A. *J. Chem. Phys.* **1965**, *42*, 245.
(46) Legrand, D. G. *J. Appl. Polym. Sci.* **1969**, *13*, 2129.
(47) Lohfink, M.; Sillescu, H., unpublished results.
(48) Angell, C. A. *J. Phys. Chem. Solids* **1988**, *49*, 863.
(49) Greet, R. I.; Turnbull, D. *J. Chem. Phys.* **1967**, *46*, 1243; *47*, 2185.
(50) Vrentas, J. S.; Duda, J. L. *J. Appl. Polym. Sci.* **1978**, *22*, 2325.
(51) Vilgis, T. A. *J. Phys. C: Solid State Phys.* **1988**, *21*, L 299.
(52) Fischer, E. W.; Hellmann, H.; Spiess, W.; Hörth, U.; Ecarius, M.; Wehrle, M. *Makromol. Chem. Suppl.* **1985**, *12*, 189.
(53) Hozumi, S.; Wakabayashi, T.; Sugihara, K. *Polym. J.* **1970**, *1*, 632.
(54) Hozumi, S. *Polym. J.* **1971**, *2*, 756.
(55) Lundberg, J. L.; Wilk, M. B.; Hayett, M. *J. Ind. Eng. Chem. Fund.* **1963**, *2*, 37.
(56) Hu, D. S.; Han, C. D.; Stiel, J. I. *J. Appl. Polym. Sci.* **1987**, 551.
(57) Zhang, J.; Wang, C. H.; Chen, Z.-X. *J. Chem. Phys.* **1986**, *85*, 5359.
(58) Zhang, J., private communication.
(59) Antonietti, M.; Fölsch, K. J.; Sillescu, H. *Makromol. Chem.* **1987**, *188*, 2317.
(60) Donth, E.-J. *Glasübergang*; WTB Bd. 271, Akademie Verlag: Berlin, 1981.
(61) Wang, C. H.; Xia, J. L. *Macromolecules* **1988**, *21*, 3519.
(62) In a more recent communication (Wang, C. H.; Xia, J. L. *Macromolecules* **1989**, *22*, 2019) the authors present diffusion coefficients of CQ in oriented PC, which appear to us even more unlikely since the anisotropy of $D_{\parallel}/D_{\perp} = 4$ reported for a PC film hot drawn to 132% extension would be much larger than the value of $D_{\parallel}/D_{\perp} = 1.6$ found for the diffusion of methyl red in an ordered nematic liquid crystal (Hervet, H.; Urbach, W.; Rondelez, F. *J. Chem. Phys.* **1978**, *68*, 2725). We have also looked for anisotropic diffusion of TTI in a sample of PC that was hot pressed (220 °C, 30 min at 2 kN and 5 min at 10 kN, cooled at ~8 K/s) and drawn at room temperature to an extension ratio of 1.7. We could detect no difference between $D_{\parallel}$ and $D_{\perp}$.[31]
(63) Gierer, A.; Wirtz, K. *Z. Naturforsch.* **1953**, *8a*, 532.
(64) McClung, R. E. D.; Kivelson, D. *J. Chem. Phys.* **1968**, *49*, 3380.
(65) Ehlich, D. Diplomarbeit, Universität, Mainz, 1984.
(66) Hu, D. S.; Han, C. D.; Stiel, L. I. *J. Appl. Polym. Sci.* **1987**, *34*, 423.
(67) Haward, R. N., Ed. *The Physics of Glassy Polymers*; Applied Science Publishers: London, 1973.
(68) Ishida, Y.; Matsuoka, S. *Polym. Prepr. (Am. Chem. Soc., Div. Polym. Chem.)* **1965**, *6* (2), 795.
(69) Haward, R. N. *J. Macromol. Sci.-Rev. Macromol. Chem.* **1970**, *C4*, 191.
(70) Kokes, R. J.; Long, F. A. *J. Am. Chem. Soc.* **1953**, *15*, 6142.
(71) D of TIP was determined for 165 and 175 °C at different concentrations. The value of $D = 2.5 \times 10^{-9}$ cm^2 s^{-1} at 165 °C is essentially based on a linear extrapolation to zero TIP concentration from two D values at 2% and 4.5% TIP in PS. Errors of less than ±20% can increase the extrapolated D value such that $\xi \leq 1$.

Registry No. *trans*-TTI, 16291-99-9; ONS-N, 61599-59-5; ONS-B, 124604-84-8; ONS-A, 124604-85-9; PS, 9003-53-6; PES, 51154-97-3; PMMA, 9011-14-7; PEMA, 9003-42-3; TNB, 7059-70-3; PC (SRU), 24936-68-3; (bisphenol A)(carbonic acid) (copolymer), 25037-45-0.